AIAA 81-4325

Effect of Deformation on Flame Spreading and Combustion in Propellant Cracks

Mridul Kumar* and Kenneth K. Kuo†
The Pennsylvania State University, University Park, Pa.

A comprehensive theoretical model was formulated to study the development of convective burning in a solid propellant crack which continually deforms due to burning and pressure loading. The effect of interrelated structural deformation and combustion processes was included in the theoretical model. The set of coupled, nonlinear, governing partial-differential equations was solved numerically. Several regions of partial crack closures were observed experimentally in narrow cracks (gap width ~450 μm). Predicted results indicate that the partial closures may generate substantial local pressure peaks along the crack, implying a strong coupling between chamber pressurization, crack combustion, and propellant deformation, especially when cracks are narrow and chamber pressurization rates are high. Predicted results for ignition-front propagation and pressure distribution are in good agreement with experimental data. Both theoretical and experimental results indicate that the maximum pressure in the crack cavity is generally higher than that in the chamber. Under the conditions studied, it was found that the initial flame-spreading process is not affected substantially by propellant deformation.

Nomenclature

A_p = cross-sectional area of the crack, m^2
a = pre-exponential factor in the nonerosive burning rate law, aP^n, (mm/s)/(atm)^n
B_x = body force, N/kg
b = covolume, m^3/kg
c_f = friction coefficient, $2\tau_w/\rho u^2$
c_p = specific heat at constant pressure, J/kg-K
d_h = hydraulic diameter of crack, m
E = total stored energy (internal and kinetic), J/kg
G_1 = relaxation modulus, Pa
$\bar{h}_c$ = local convective heat-transfer coefficient, W/m^2-K
$\bar{h}_{cp}$ = local convective heat-transfer coefficient over propellant surface, W/m^2-K
$\bar{h}_{cw}$ = local convective heat-transfer coefficient over nonpropellant port wall, W/m^2-K
K = bulk modulus, Pa
K_e = erosive-burning constant, m^3-K/J
L = length of crack, m
M_w = molecular weight, kg/kmole
n = pressure exponent in nonerosive burning rate law
P = pressure, Pa
Pr = Prandtl number
$\mathcal{P}_b$ = burning perimeter, m
$\mathcal{P}_w$ = wetted perimeter of the port, m
R = specific gas constant for combustion gases, N-m/kg-K
Re = Reynolds number
r_b = burning rate of solid propellant, including erosive-burning contribution, m/s
T = temperature (without subscript, static gas temperature), K
T_{af} = average film gas temperature, $(T+T_{ps})/2$, K
T_f = adiabatic flame temperature of solid propellant, K
T_{pi} = initial propellant temperature, K
T_{ps} = propellant surface temperature, K
T_{ws} = nonpropellant wall surface temperature, K
t = time, s
u = gas velocity, m/s
V_k = coefficient in viscosity-temperature relation [see Eq. (15)]
v_{gf} = velocity of propellant gas at burning surface, m/s
x = axial coordinate, measured from crack entrance, m
x_L = position at end of crack, m
x_p = axial distance along crack at which propellant begins, m
y = transverse coordinate, measured from propellant surface into solid, m
α = thermal diffusivity, m^2/s
β = erosive-burning exponent
γ = ratio of specific heats
δ = gap width of crack, m
ϵ = strain tensor
ϵ_s = surface roughness, m
λ = thermal conductivity, W/m-K
σ = stress tensor
μ = gas viscosity, kg/m-s
ρ = density (without subscript, gas density), kg/m^3
τ_w = shear stress on port wall
τ_{xx} = normal viscous stress
θ_w = angle measured, in a counterclockwise direction, at lower side of propellant

Subscripts

c = chamber conditions
eff = effective
g = gas
i = initial value
ign = ignition condition
pr = propellant
ps = propellant surface

Introduction

HIGH-ENERGY propellants, which are used to obtain increased specific impulse in rocket motors, generally contain high solids loading of energetic materials, e.g., cyclotertramethylenetetranitramine (HMX). As the density of solids in the propellant is increased, the probability that cracks and flaws will develop in the propellant grain is also increased. Defects in propellant grains can originate during manufacture, storage, or handling, during ignition and combustion, or during loading of different segments of a segmented rocket.

Received Dec. 1, 1980; revision received April 24, 1981.

*Assistant Professor, Dept. of Mechanical Engineering. Member AIAA.

†Professor, Dept. of Mechanical Engineering. Associate Fellow AIAA.

Cracks in solid propellant grain can provide additional surface area for combustion. The phenomenon of rapid flame propagation into propellant cavities together with subsequent rapid regression is called convective burning. The convective burning rate often exceeds the normal (conductive) burning rate. Mechanical deformation and crack propagation may result when combustion processes inside the crack produce pressure much higher than the designed maximum pressure. If local pressure rise due to gasification is sufficiently rapid, it may produce strong compression waves, or even shock waves, which can initiate detonation. The generally understood mechanism of transition from deflagration to detonation (DDT) is given in Ref. 1. Since propellant grains with flaws or cracks have large burning surface areas, they possess a higher propensity for transition to detonation.

Convective burning inside a crack involves several interdependent processes such as: pressure wave phenomenon; convective heating of the surface of the propellant crack and subsequent flame propagation along the crack; pressurization of the crack cavity due to burning, which may result in flow reversal when the pressure inside the crack exceeds that of the chamber; change in the crack geometry due to burning, as well as mechanical deformation caused by pressure loading; and propagation of the crack due to regression and mechanical fracture. Parameters which may significantly affect the combustion process are chamber pressure and pressurization rate, geometry of the crack, erosive-burning effects due to high gas velocities, physicochemical properties of the propellant, composition of the igniter gas, and initial and boundary conditions.

This paper deals with the formulation of a comprehensive theoretical model, which includes the effect of propellant deformation to predict flame-spreading and combustion processes during the development of convective burning in solid propellant cracks. Predicted results are also compared with some of the experimental investigations[2,3] conducted by the authors for model validation.

Since the propellant is deformable, burning inside a solid propellant crack is basically a coupled solid mechanics and combustion phenomenon. Both burning rate and mechanical deformation are governed by pressures acting on the crack surfaces. On the other hand, a change in gap width or geometry will cause variation of pressure distribution, which in turn will strongly influence deformations along the crack and stress concentration at the crack tip.

Convective burning inside a solid propellant crack has been a subject of interest in recent years. An extensive literature review in this area was recently conducted by Bradley and Boggs.[4] Belyaev et al.[5] have compiled most of the recent Russian work on convective burning and DDT. Both theoretical and experimental studies in the area of crack combustion have been conducted at The Pennsylvania State University.[6-10] Convective-burning studies can be subdivided into two broad categories, onset of convective burning and development of convective burning. The present study is restricted to the development of convective burning in isolated propellant cracks. The following paragraphs list some of the important research conducted in this area.

Experimental and theoretical studies on the development of convective burning are limited. Belyaev et al.[11,12] made preliminary experimental investigations on the development of combustion in single pores. Kuo et al.[6] developed a detailed theoretical model for predicting the development of convective burning in isolated propellant cracks; this model,[6] however, did not include mechanical deformation of the crack during development of convective burning. Kim[13] studied the possibility of shock to detonation transition in propellant cracks using the model of Kuo et al.[6] and an extremely simplified, one-dimensional, elastic model for propellant deformation. Pilcher[14] also reported some computations conducted on a deformable crack, but gave no details.

High pressures present in the crack during development of convective burning, as well as associated mechanical deformation and stress concentrations, may lead to crack propagation. Most of the earlier work in the area of crack propagation was done in the USSR.[15-17] Kirsanova and Leipunskii[15] examined the mechanical stability of propellant cracks, using steady-state approximations, and assuming the material to be elasto-brittle. A greatly improved analytical model for the same problem was formulated by Cherepanov.[16] The propellant material was assumed to be elasto-plastic and the deformation process to be quasistatic. However, Cherepanov did not solve the governing set of equations and, therefore, did not present any results. Belyaev et al.[17] proposed modifications to the Kirsanova and Leipunskii[15] model, pointing out some of its limitations. They noted that an elasto-brittle material model cannot describe the viscoelastic character typical of solid propellants.

Some of the earliest works in the United States on the critical nature of cracks and debonds were conducted by Jacobs et al.,[18-20] assuming instantaneous flame spreading throughout the crack. The propellant was considered to be linear viscoelastic. Other related studies on crack combustion have been reported.[21-24] Takata and Wiedermann[23,24] have been investigating initiation of detonation in a propellant crack by introducing the effect of stress wave interaction with the crack boundary, under the assumption that a foam layer is present on the propellant surface during combustion. The propellant was considered to be linear, isotropic, elastic material that does not yield or fail.

Numerous studies, based purely on solid mechanics considerations (for example, Refs. 25-34), have been conducted on crack propagation. All are based on quasistatic crack propagation in viscoelastic material and use the concept of local energy dissipation at the crack tip. Work on dynamic crack propagation is currently underway, with Swanson[34] reporting some progress in this area. However, there is at present no theoretical model capable of realistically predicting stress concentrations at the tip of a burning crack, which is a necessary input for all crack-propagation theories.

It is apparent that a theoretical model is needed to predict the development of convective burning, while also taking into account the effect of mechanical deformation. Such a model would also be extremely useful in making realistic predictions of crack propagation; at present, these predictions are based purely on solid mechanics considerations. Even though this investigation will not attempt to study crack propagation caused by mechanical fracture at the tip, the analysis and program developed here can be extended easily for such a study.

Specific objectives of this study are:

1) To develop a theoretical model to study ignition, flame spreading, and convective burning in a solid propellant crack which continually deforms due to burning and pressure loading.

2) To study the effects of such parameters as chamber pressurization rate, dP/dt, and crack-gap width on the flame-spreading and combustion process in propellant cracks.

3) To test the validity of the theoretical model by comparing predicted results with experimental data.

Actual propellant defects may consist of several irregularly branched cracks. However, because of the complexity of physical processes involved in the study of combustion in propellant cracks, and for mathematical tractability, this investigation is limited to a single isolated crack.

Analysis

Description of Physical Model

A schematic diagram of the physical model chosen to simulate a propellant crack is shown in Fig. 1. The location of the crack is normal to the main flow direction in the combustion chamber or in a rocket motor. The current analysis is

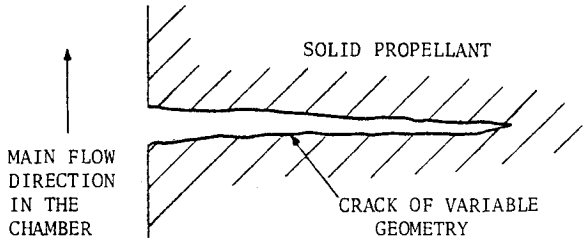

Fig. 1 Schematic diagram of the physical model.

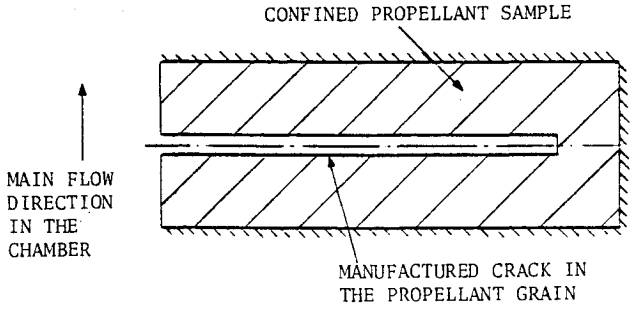

Fig. 2 Schematic diagram of cracks used in experiments.

applicable to a crack of variable geometry. However, in order to closely simulate the assumptions of the physical model, and to facilitate the manufacture of a reproducible propellant crack, specimens used in the experimental study were of uniform rectangular cross section. A schematic diagram of the propellant crack geometry used in the experimental investigation is shown in Fig. 2.

As hot combustion gases flow through the main chamber, a portion of the gases is driven into the crack because of the pressure gradient; and as hot gases flow over the propellant crack, energy is transferred from the gas to the propellant. The rate of heat transfer to the propellant depends upon the local temperature, velocity, and density of the gas, and on the temperature of the propellant surface. The heat transfer may cause the propellant to ignite. As additional gases are driven into the crack, density and velocity increase further, resulting in faster flame propagation along the crack. As the ignition front moves downstream, more hot gases are generated by combustion of the propellant surface, causing local pressure to increase. At the same time, the deformation of the propellant will also alter the pressure. The net result of these two opposing and interdependent phenomena determines local pressure.

Basic Assumptions

The following basic assumptions are made in the derivation of the theoretical model.

1) The gas-phase reaction zone is considered quasisteady. In other words, the relaxation time associated with the flame is much shorter than that associated with transient pressure variation; therefore, the flame adjusts itself immediately to chamber conditions.

2) The deformation of the propellant is quasisteady; that is, the mechanical deformation of the propellant can be obtained by using a static analysis.

3) Flame stand-off distance is small when compared to crack-gap width.

4) The bulk flow of the gases in the pore is considered to be one dimensional.

5) Gases present in the propellant crack obey the Nobel-Abel gas law.

6) The propellant surface temperature is uniform, and thermal properties of the propellant are constant.

7) The propellant can be represented by a linear viscoelastic material model; the material is assumed to be isothermal, homogeneous, and isotropic. The propellant grain is two dimensional, with no mechanical fracture at the crack tip.

The validity of assumptions 1 and 2 can be demonstrated by comparing the characteristic times associated with pressure variation, gaseous flame zone, and compression-wave propagation through the propellant grain. In the crack combustion experiments, the typical time associated with the pressure excursion, τ_p, is in the order of 1 ms. The characteristic time associated with the gaseous flame, τ_g, is in the order of 0.01 ms. The time associated with the compression wave, τ_c, is in the order of 5 μs, where τ_c is based on web thickness and bulk modulus.

Since τ_g and τ_c are both $\ll \tau_p$, the quasisteady assumption of the flame zone and mechanical deformation is valid. The value of τ_c calculated from the shear modulus will be an order of magnitude higher; however, it will still be smaller than τ_p. Assumption 3 is reasonable for ammonium perchlorate (AP) based composite solid propellants in the pressure range of interest. Even though the heat release zone is distributed, the diffusion flame stand-off distance is usually in the order of 50 μm, and is small in comparison to the gap width (gap widths are in the order of 500 μm in the present experimental investigation).

Assumption 4 is justified for the crack dimensions used in this investigation. The crack length to hydraulic diameter ratio was approximately 100. The dense gas relation (assumption 5) adequately describes the departure from the ideal gas law at high pressures. Assumption 6, employed for mathematical simplicity, allows the use of a one-dimensional transient heat conduction equation for the solid. Since the thermal wave penetration depth is of the same order of magnitude as the oxidizer particle size of the propellant, the actual heat transfer process is three dimensional. However, researchers in the field have not yet investigated the three-dimensional treatment of the heat conduction process in composite solid propellants because of the complexities associated with the three-dimensional structure of oxidizer crystals and fuel binder, and the fact that numerical solutions are cumbersome and time consuming.

Most of the solid propellants can be satisfactorily characterized by a viscoelastic material model.[25-34] For the sake of simplicity, the viscoelastic material model was assumed to be linear. Even though the assumption of isothermal condition for material response is not strictly accurate, it is a good approximation since the thermal wave penetration depth is less than 100 μm. Fracture of the propellant at the crack tip was considered beyond the scope of the present investigation since it is a vast subject in itself. The viscoelastic nature of the material, i.e., the time dependence of the relaxation modulus, may not be very significant during the period of experimental test firings of this study because the stress relaxation time is much greater than the transient pressure variation time. Indeed, the analysis and model developed here are applicable to a wide variety of operating conditions, and are not limited simply to the experimental test conditions of the present study.

In this analysis, ignition is defined as the attainment of a critical temperature at the propellant surface. It is assumed that no solid or gas-phase reaction takes place before onset of ignition. The tacit assumption here is that there is little time between the attainment of a critical surface temperature and the reaction between the fuel and the oxidizer species to cause ignition. Flame spreading is postulated to be successive ignition of adjacent propellant surface elements.

Governing Equations

The unsteady, variable area, one-dimensional gas-phase conservation equations for reacting compressible fluid flow are given first, followed by the other governing equations.

Mass conservation

$$\frac{\partial(\rho A_p)}{\partial t}+\frac{\partial(\rho u A_p)}{\partial x}=r_b\rho_{pr}\mathcal{P}_b \tag{1}$$

Moment conservation

$$\frac{\partial}{\partial t}(\rho u A_p)+\frac{\partial}{\partial x}(\rho A_p u^2)=-A_p\frac{\partial P}{\partial x}+\cancel{\frac{\partial}{\partial x}(A_p\tau_{xx})}$$

$$-\mathcal{P}_w\tau_w\cos\theta_w+\rho A_p B_x-(\rho_{pr}r_b\mathcal{P}_b)v_{gf}\sin\theta_w \tag{2}$$

Energy conservation

$$\frac{\partial}{\partial t}(\rho A_p E)+\frac{\partial}{\partial x}(\rho A_p u E)=\cancel{\frac{\partial}{\partial x}\left(\lambda A_p\frac{\partial T}{\partial x}\right)}-\frac{\partial}{\partial x}(A_p P u)$$

$$+\cancel{\frac{\partial}{\partial x}(\tau_{xx}A_p u)}+\rho_{pr}r_b\mathcal{P}_b h_f-\bar{h}_{cp}\mathcal{P}_b(T-T_{ps})$$

$$+B_x\rho A_p u-\bar{h}_{cw}(\mathcal{P}_w-\mathcal{P}_b)(T-T_{ws}) \tag{3}$$

An order of magnitude analysis was made; terms crossed with arrows in Eqs. (2) and (3) were found to be much smaller than the others, and hence were dropped.

Equation of state for the gas-phase

$$P[(1/\rho)-b]=RT \tag{4}$$

Equation for stress equilibrium in the solid-phase (neglecting body force)

$$\partial\sigma_{ij}/\partial x_j=0 \tag{5}$$

Constitutive law for linear viscoelastic material

$$\sigma_{ij}(t)=\int_{-\infty}^{t}G_1(t-\tau)\frac{\mathrm{d}}{\mathrm{d}\tau}\epsilon_{ij}(\tau)\,\mathrm{d}\tau$$

$$-\frac{1}{3}\delta_{ij}\int_{-\infty}^{t}G_1(t-\tau)\frac{\mathrm{d}\epsilon_{kk}}{\mathrm{d}\tau}\,\mathrm{d}\tau+\delta_{ij}K\epsilon_{kk} \tag{6}$$

The transient heat conduction equation for the solid-phase, before ignition

$$\frac{\partial T_{pr}}{\partial t}=\alpha_{pr}\frac{\partial^2 T_{pr}}{\partial y^2} \tag{7}$$

The initial and boundary conditions for Eq. (7) are

$$T_{pr}(0,y)=T_{pi} \tag{8}$$

$$T_{pr}(t,\infty)=T_{pi} \tag{9}$$

$$\frac{\partial T_{pr}}{\partial y}(t,0)=-\frac{\bar{h}_c(t)}{\lambda_{pr}}[T(t)-T_{ps}(t)] \tag{10}$$

After rearranging the gas-phase conservation equations and making some simplifications, velocity-variation, temperature-variation, and pressure-variation equations were obtained. These equations were found to be totally hyperbolic in nature.[35] Gas-phase and solid-phase equations were solved separately. Details of the numerical scheme for solving gasdynamics equations and solid mechanics equations are given in a later section.

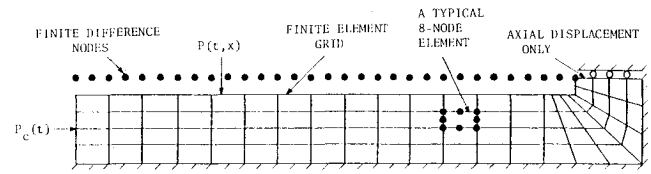

Fig. 3 Boundary conditions, finite-element grids, and finite-difference nodes for a test specimen.

Initial and Boundary Conditions

Initial and boundary conditions must be specified in order to complete the theoretical formulation. The three initial conditions necessary for the solution were specified as

$$u(0,x)=u_i,\quad T(0,x)=T_i,\quad P(0,x)=P_i \tag{11}$$

The number of physical boundary conditions that can be specified depends upon flow conditions at the opening of the crack. When gases flow into the crack at a subsonic speed, boundary conditions are

$$P(t,0)=P_c(t),\quad T(t,0)=T_c(t),\quad u(t,x_L)=0 \tag{12}$$

When gases flow out of the crack, and the outflow is subsonic, only one boundary condition can be specified at the crack opening. Boundary conditions are given as

$$P(t,0)=P_c(t),\quad u(t,x_L)=0 \tag{13}$$

When the gases flow out of the crack supersonically, no boundary condition can be specified at the crack entrance. In such a case, the only specified boundary condition is

$$u(t,x_L)=0 \tag{14}$$

The extraneous boundary conditions needed to solve the equations are obtained by using the characteristic equations.[35]

A schematic diagram of the boundary conditions for two-dimensional structural analysis is shown in Fig. 3. Because of the symmetry of the crack specimens (see Fig. 2), only half of the crack is considered. All surfaces of the propellant are either pressure loaded or have fixed boundaries. The propellant surface exposed to the chamber experiences the chamber pressure $P_c(t)$, whereas the surface along the crack experiences the local pressure along the crack, $P(t,x)$. Due to the symmetry along the centerline of the crack, the propellant boundary at the tip is allowed to have deformations only along the axial direction. Boundaries along the surface of the propellant in contact with the brass mold are assumed to be fixed.

Empirical Correlations

To close the system of governing equations, empirical correlations are needed for the heat-transfer coefficient, drag-coefficient, and burning-rate law. The correlation for the local convective heat-transfer coefficient $\bar{h}_c$ is deduced from the Dittus-Boelter correlation for flow in a pipe. The effect of the entrance region is taken into account by using a power function of length-to-hydraulic diameter ratio.[36,37] The dependence of viscosity on temperature was included, using Svehla's expression[38] for viscosity of air at high temperature. Bartz[39] had shown good comparisons between Svehla's equation and published NBS data.[40] Svehla's expression for viscosity is

$$\mu=V_k T^{0.65}\ \text{where}\ V_k=8.699\times10^{-8}M_w^{0.5} \tag{15}$$

For turbulent flow, the final expression for $\bar{h}_c$ is[36,37]

$$\bar{h}_c = 0.0346 Pr^{-0.6} c_p (Pu/R)^{0.8} V_k^{0.2} T_{af}^{-0.67} (x d_h)^{-0.1} \quad (16)$$

The Prandtl number in Eq. (16) is calculated from Svehla's equation[38]

$$Pr = \gamma/(1.77\gamma - 0.45) \quad (17)$$

The correlation for the friction coefficient for turbulent flow used in this study is[36,37]

$$c_f = \frac{0.4491 (d_h/x)^{0.1}}{\left\{ \ell n \left[\frac{\epsilon_s/d_h}{3.7} + \frac{1.46 R V_k T_{af}^{1.65} (d_h/x)^{0.05}}{P u d_h c_f^{0.5}} \right] \right\}^2} \quad (18)$$

where ϵ_s/d_h is the relative equivalent sand roughness. This expression is a modified form of the well-known Colebrook formula[41,42] for turbulent flow in pipes with roughness. Entrance effects are taken into account by modifying the friction coefficient by a power function of the distance-to-diameter ratio. After the propellant surface begins to burn locally, the value of the friction coefficient is set at zero, due to the attenuation of wall shear stress caused by surface blowing.

The burning-rate expression is obtained from the strand-burning rate data and is given by

$$r_b = aP^n \quad (19)$$

The effect of erosive burning is taken into account by using either the erosive-burning augmentation factor obtained by Razdan and Kuo,[43]

$$r_b = aP^n [1 + K(P)^{n_p} (u)^{n_u}] \quad (20)$$

or the Lenoir-Robillard burning-rate formula,[44]

$$r_b = aP^n + K_e \bar{h}_c \exp(-\beta r_b \rho_{pr}/u\rho) \quad (21)$$

Numerical Scheme for Gasdynamics Equations

An implicit finite-difference scheme was used to solve the nonlinear coupled partial-differential equations. A central-difference method was used for the derivatives at the interior nodes. The predictor-corrector method was used to handle the nonlinear nature of the governing equations. A quasilinearization method was used to linearize the inhomogeneous terms of the governing equations. The set of finite-difference equations thus obtained is solved simultaneously, using a block tridiagonal matrix inversion method.

Six boundary conditions are required when the central-difference method is used for spacewise derivatives; the difference equations for the first-order spatial derivative obtained by using this method correspond essentially to the second-order partial differential equation.[45] The extraneous boundary conditions needed for the solution of the finite-difference equations are derived from the compatibility relationships at the boundaries. These relationships were obtained by transforming the governing hyperbolic equations into their characteristic form. The equations determining the extraneous boundary conditions are all first-order, ordinary differential equations. They are simultaneously integrated, using a fourth-order Runge-Kutta integration technique.

The extraneous boundary conditions used are as follows. When the gas flows into the crack, the three extraneous boundary conditions required [in addition to the physical boundary conditions, Eq. (12)] are velocity at the crack entrance, and pressure and temperature at the crack tip. When the gas flows out of the crack subsonically, the four necessary extraneous boundary conditions are pressure and velocity at the crack entrance, and pressure and temperature at the crack tip. When the gas flows out of the crack supersonically, the five required extraneous boundary conditions are pressure, temperature and velocity at the crack entrance, and pressure and temperature at the crack tip.

Numerical Scheme for Solid-Phase Heat Equation

The governing partial-differential equation for the solid phase, Eq. (7), was solved by using an implicit finite-difference technique with a variable mesh system. The variable grid spacing provides finer grid spacing near the surface. The central-difference method was used to approximate both time and spatial derivatives. The resulting set of simultaneous algebraic equations was solved by using a standard tridiagonal matrix inversion method.

Numerical Scheme for Structural Analysis

Mechanical deformation of the propellant was obtained by using a general purpose structural analysis program, the nonlinear finite-element analysis program (NFAP).[46] This is an extended version of the nonlinear structural analysis program (NONSAP).[47,48] Since NONSAP is well-documented and easily accessible, details of the numerical procedure used in NONSAP will not be repeated here. NFAP was modified and consolidated to suit the needs of the present study, and for efficiency of computational storage. Three major features added to the numerical formulations are: 1) modeling of the viscoelastic material behavior, 2) simulation of the ablating boundary, and 3) treatment of the material response by an interpolation scheme. Details of this formulation can be found elsewhere.[8,49]

To test the numerical procedure developed in this section, the modified version of NFAP was used to compute several viscoelastic problems for which exact solutions are known. The agreement between NFAP solutions and exact solutions is excellent. Details of these comparisons are given in Ref. 49.

Numerical Procedure

Of the several interdependent gasdynamics and solid mechanics processes that may influence combustion behavior in a propellant crack, the coupling between the pressure along the crack and the structural deformation was considered to be the most important. Other coupled processes, such as thermal stresses due to the temperature gradient in the solid, variation in burning rate due to compression of the propellant, etc., were considered to be of secondary importance and were ignored in the present analysis.

The general computation procedure is as follows. Pressure is calculated by the gasdynamics portion of the computer program at each nodal point on a one-dimensional grid along the length of the crack. The convective-burning analysis of the crack combustion incorporates the crack-geometry variation caused by both mechanical deformation and mass loss through gasification of the propellant surface. Once the gas-phase equations are solved, the pressures and burning rates along the crack are calculated for a particular time t, program control is transferred to the structural analysis (NFAP) portion of the combined program. NFAP reformulates the geometry because of the material loss, and updates the stiffness matrix for the new time-step. Surface elements of the finite-element mesh are loaded with the pressure obtained through the gas-phase equations. Propellant deformation is calculated in NFAP using a static analysis at time t. General stress-strain equations are solved using a plane-strain analysis; this is congruous to the experimental test configuration. The transient nature of the pressure loading is considered by using a static analysis at incremental time steps.

Figure 3 also includes the finite-element grid used for the structure analysis, and the finite-difference nodes used for the gas-phase solutions. The configuration is compatible with the

geometry considered in the theoretical model, as well as with that used in the experiments. Two-dimensional, eight-node, isoparametric, quadrilateral elements were used to model a sample crack. Because of symmetry, only half of the crack needs to be considered. Of the eight nodes in an element, four are located at the corners, and one at the midpoint of each side.

Results and Discussion

Experimental Results

Figure 4 shows a schematic diagram of the test configuration used for detailed observation of the flame front. The crack is formed between a propellant slab and an inert, transparent plexiglass window; the crack is perpendicular to the direction of flow in the main chamber. This type of configuration provides direct (front-view) observation of the ignition front propagation and burning propellant surface, even in the case of very narrow cracks. Most of the experimental results were obtained with cracks formed by cutting a slot of desired width in a propellant slab (see Fig. 2). Details of the experimental setup and experimental results are given in Refs. 2 and 3. The entrance of the crack gap is rounded to facilitate gas penetration.

Figure 5 presents a sequence of pictures obtained from a test performed on a 183-mm long, narrow crack ($\delta \sim 455$ μm); the framing rate in this case was 36,700 pictures /s. The crack configuration is the same as that shown in Fig. 4. It was observed that when the width of the crack gap is very small (<500 μm) partial closure of the crack occurs due to propellant deformation. This partial closure first appears near the entrance. As time progresses, the closure region moves downstream and a second partial closure region develops near the entrance. This process continues; at times, three or four such partial closures are observed simultaneously (for initial gap widths of the order of 450 μm). Usually, at the moment when the third closure develops at the entrance, the second and first are located, respectively, at approximately 20 and 50% of the crack length from the entrance. Later, as the combustion becomes more pronounced, partial closure regions disappear as a result of both propellant regression and higher pressure in the cavity.

The entire process is believed to be the result of deformation caused by high pressure acting on the propellant surface exposed to the chamber, and by complex interaction between propellant deformation and pressure distribution in the crack cavity. Propellant surfaces exposed to the chamber are compressed by the high chamber pressure, with the result that the propellant is pushed into the crack. Since pressure increases faster in the chamber than in the crack during this initial pressure transient, the propellant is pushed toward the region of lower pressure inside the crack. Mechanical deformation of the propellant causes narrowing of the crack gap, and consequently results in local crack closure.

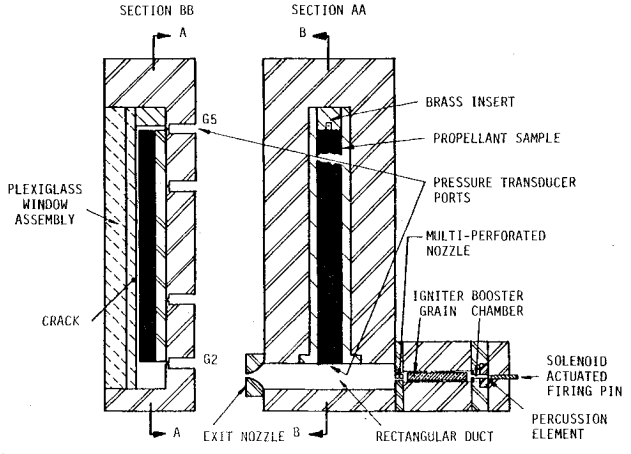

Fig. 4 Schematic diagram of configuration used for detailed observation of the flame front.

Theoretical Predictions and Comparisons

The important physical properties of the two propellants studied are given in Table 1. Numerical values of input variables used in the predictive program are listed in Table 2. The recorded pressure-time trace near the crack entrance was used as an input. The temperature of hot gases in the chamber was assumed to be the adiabatic flame temperature of product gases from the igniter. An estimate of heat loss indicated that it is less than 3% of the chemical heat release; therefore, this assumption is justified. The flame temperature for propellant A was obtained from Price[50] of Navel Weapons Center; for the other propellant, it was computed from the CEC 72 thermochemistry program.[51]

Calculated pressure distributions at various times in a typical test case for propellant A are shown in Fig. 6. Results are presented only for the period of initial rapid pressure rise, since that is the region of interest for this study. The average pressurization rate at the crack entrance was 1.75×10^5 atm/s. During the initial period, a traveling pressure wave is present in the crack cavity. This wave moves toward the crack tip and is reflected from the tip, resulting in higher pressure near the tip at $t = 0.6$ ms. As time progresses, the overall pressure in the crack cavity continues to rise. This is the result of a combination of two simultaneous processes: 1) a continuous increase in chamber pressure during this period, and

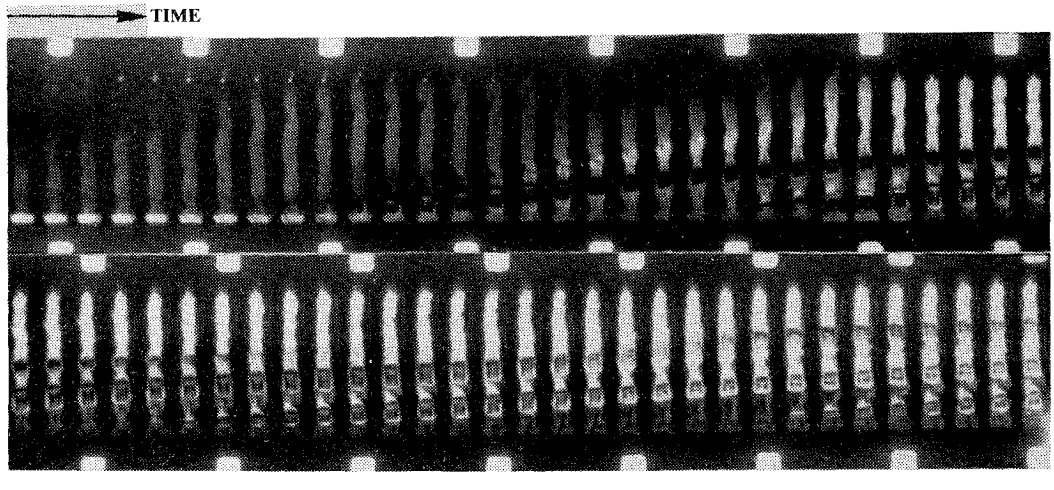

Fig. 5 A sequence of photographs showing crack-gap closures, $L = 183$ mm and $\delta = 455$ μm. Framing rate = 36,700 pictures/s.

Table 1 Propellant properties

Propellant type	A	B
Composition	AP-based	AP/PBAA-EPON
Weight percent of oxidizer	...[a]	75
Average particle size, d_{AP}, μm	...[a]	76
Pre-exponential factor in Saint Robert's burning rate law, a, mm/s/(atm)^n	1.62	0.9591
Pressure exponent in Saint Robert's burning rate law, n	0.4108	0.41
Flame temperature, T_f, K	3000	1920
Propellant density, kg/m^3	1710	1600

[a] AP weight percent and particle size for propellant A not avialable to the authors.

Table 2 Numerical values of input variables

Variable	Units	Propellant A	Propellant B
x_p	mm	0.0	0.0
x_L	mm	195.0	195.0
B_x	N/kg	0.0	0.0
b	m^3/kg	1.0×10^{-3}	1.0×10^{-3}
M_w	kg/kmole	26.10	20.38
γ	–	1.21	1.26
ρ_{pr}	kg/m^3	1710	1600
λ_{pr}	W/m-K	0.335	0.21
α_{pr}	m^2/s	0.18×10^{-6}	0.11×10^{-6}
ϵ_s/d_h	–	0.025	0.025
T_f	K	3000	1920
T_{ign}	K	850	850
T_i	K	295	295
a	(mm/s)/(atm)^n	1.62	0.9591
n	–	0.4108	0.41
K_e	m^3-K/J	1.67×10^{-7}	–
β	–	53	–
T_c	K	1920	1920
G_1	atm	$14.4+136e^{-0.095t}$	$14.4+136e^{-0.095t}$
K	atm	47,619	47,619
K^a	(MPa)$^{-n_p}$(m/s)$^{-n_u}$	–	2×10^{-4}
$n_p{}^a$	–	–	0.705
$n_u{}^a$	–	–	1.252

[a] Defined in Eq. (20).

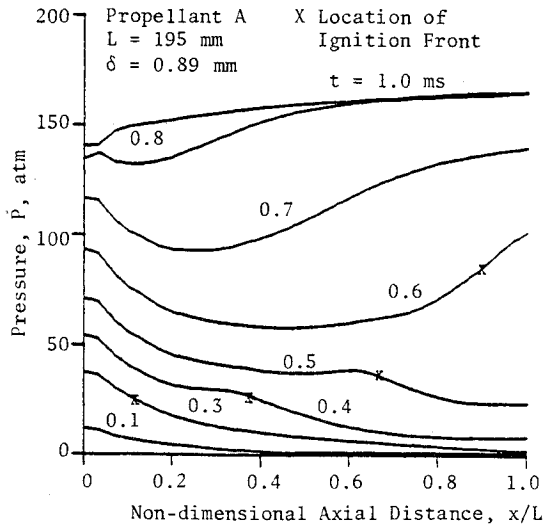

Fig. 6 Calculated pressure distribution at various times.

2) mass addition due to burning of the crack walls. After about 0.8 ms, the pressure in the crack becomes more uniform because the rate of increase of chamber pressure has become quite small and the ignition front has propagated to the tip. It should be noted that as time passes, maximum pressure in the crack cavity becomes higher than that in the chamber.

Predicted velocity distributions at various times are plotted in Fig. 7. At $t=0.1$ ms, velocity in the latter half of the crack

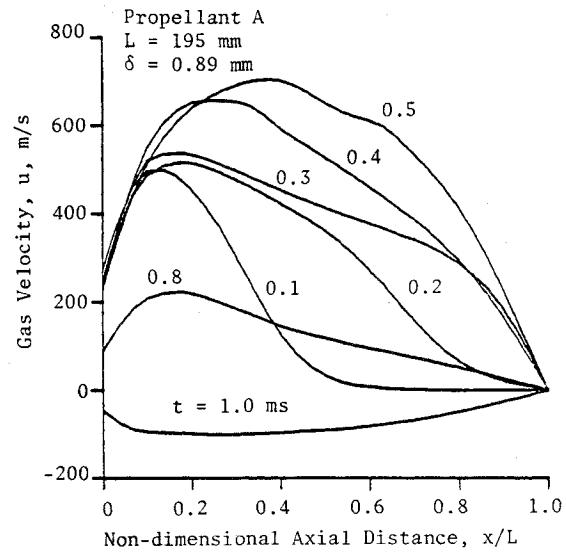

Fig. 7 Calculated velocity distribution at various times.

is almost zero. Because the initial favorable pressure gradient causes the gases to accelerate, the gas velocity at any axial location increases continuously until $t=0.5$ ms. The adverse pressure gradient generated by compression wave reflection at the crack tip causes the gases to decelerate. Since velocities continue to decrease after 0.5 ms, only one velocity distribution between 0.5 and 0.1 ms is shown in Fig. 7 to avoid confusion. At 1.0 ms, velocity in the entire crack is negative, i.e., gases flow out of the crack because pressure throughout the cavity is higher at that time than the pressure in the chamber.

Variation in the port height (≡half of the gap width) at various times is shown in Fig. 8. The initial geometry of the crack is indicated by the dashed line. Because of the rounding of the crack entrance, the gap width at the entrance is large. During the initial period, the high chamber pressure acting on the crack surface exposed to the chamber causes the propellant near the crack entrance to be pushed inside, resulting in a decreased port height near the crack entrance at $t=0.2$ ms. Later, at $t=0.6$ ms, there are two minimum gap widths; the second is caused by the deformation pattern associated with compression wave reflection in the gas phase (see Fig. 6). The deformation near the closed end is large because the pressure near the crack tip is the highest at $t=0.6$ ms. As time progresses, the pressure in the cavity exceeds that in the chamber, and the propellant continues to burn; the net result is an increase in the port height throughout the crack at 1.0 ms.

Comparisons of predicted and measured pressure-time traces at $x=48$, 138, and 188 mm are shown in Figs. 9, 10, and 11, respectively. The predicted values are in good agreement with the experimental data. The steepening of the pressurization as it moves along the crack is evident from both predicted traces and experimental data. The effect of increased pressurization is most pronounced near the tip of the crack. This is due to the combined effect of coalescence of the compression waves and steepening of the pressure front caused by gasification of the propellant behind the front.

Comparison of predicted and measured ignition-front locations for various pressurization rates is shown in Fig. 12. It can be seen that the model predicts the location of the ignition front quite well except very close to the tip. Near the tip region, the model overpredicts deceleration of the ignition front. This is believed to be caused by the one-dimensional assumption in the model; the one-dimensional assumption is inadequate to describe the flow near the tip. Since the calculated velocities near the tip are small (see Fig. 7), both the gas temperature and heat transfer coefficient are low; heat transfer to the propellant is, therefore, quite small. In an

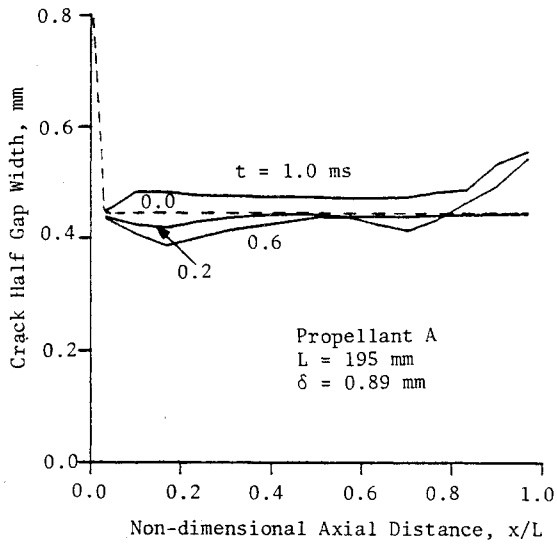

Fig. 8 Calculated variations in port height.

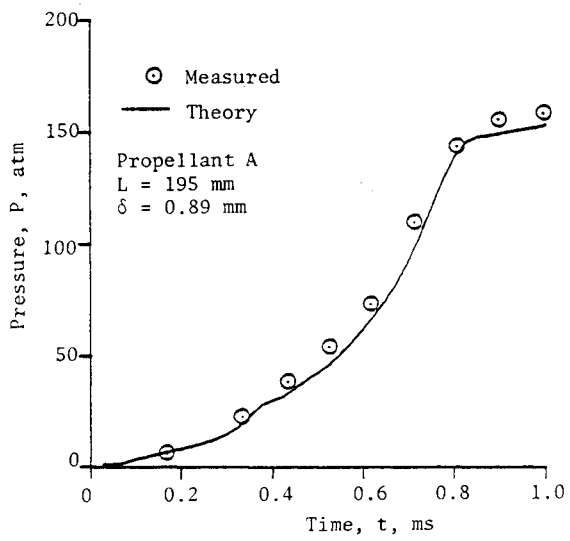

Fig. 9 Comparison between predicted and measured pressure-time traces at $x = 48$ mm.

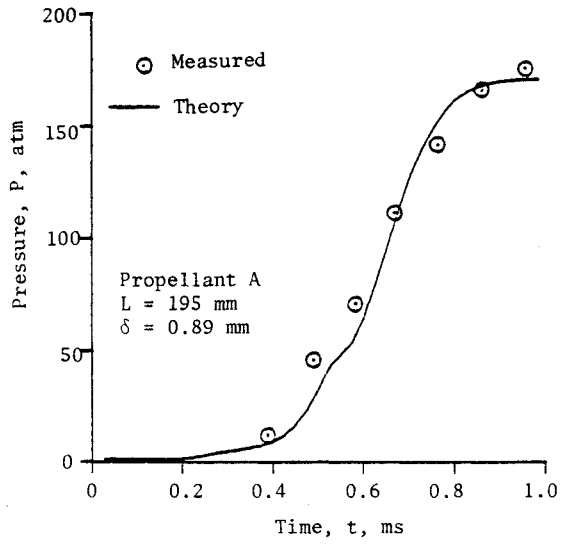

Fig. 10 Comparison between predicted and measured pressure-time traces at $x = 138$ mm.

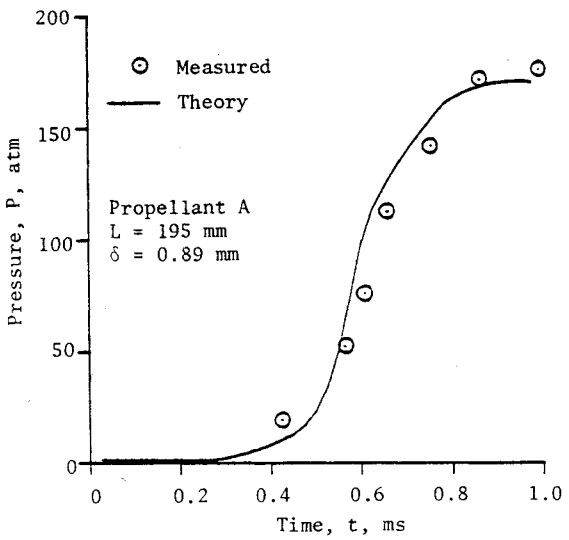

Fig. 11 Comparison between predicted and measured pressure-time traces at $x = 188$ mm.

actual case, the presence of a secondary flow near the closed end will produce a higher rate of heat transfer to the propellant, resulting in less pronounced flame front deceleration. It is believed that the discrepancy between predicted and measured ignition-front locations near the tip of the crack can be alleviated if the effect of enhanced heat transfer near the closed end can be incorporated into the model. Under the conditions studied, it should be noted that the initial flame-spreading process is not affected substantially by propellant deformation.

Figure 13 shows calculated pressure distributions at various times for a case in which propellant deformation becomes very important. The chamber pressurization rate for this case was 5×10^5 atm/s and the initial gap width was 0.89 mm. Only those curves of interest are shown in the figure and, for ease of explanation, they are not superimposed. Before 0.475 ms, the crack gap at the entrance is extremely small (partially closed). Pressure acting on the side wall exposed to the chamber and near the crack entrance cause the partial gap closure to move downstream. Area reduction and continued gasification result in a pressure peak near $x/L = 0.17$ (at 0.475 ms). At 0.5 ms, two regions of partial gap closures are obtained, resulting in pressure peaks at $x/L = 0.1$ and 0.27, respectively. As the pressure peak moves downstream, another gap closure develops near the entrance at 0.525 ms. This type of process continues, as shown by the distributions at $t = 0.525$, 0.55, and 0.575 ms. The predicted movement of the partial gap closure is qualitatively very similar to that observed experimentally (see Fig. 5).

Results obtained indicate that closure of the crack gap, which may occur initially at the crack entrance because of small gap widths and high chamber pressures, may propagate along the crack and result in local pressure peaks. The gap closure is not observed in cracks with large gap widths or at low chamber pressures because propellant deformation under these conditions is small and does not affect combustion substantially. Gap closures and resulting pressure peaks can strongly influence convective burning in the crack and may contribute to deflagration-to-detonation transition.

Summary and Conclusions

This research program was undertaken to investigate the development of convective burning in solid propellant cracks which continually deform due to burning and pressure loading. Both theoretical and experimental methods were employed to study flame spreading and combustion in propellant cracks. In the theoretical model, the effect of interrelated structural deformation and combustion

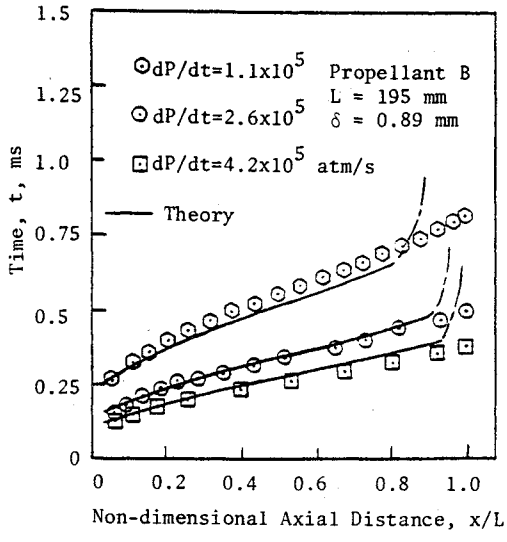

Fig. 12 Comparison between predicted and measured location of the ignition front for various pressurization rates.

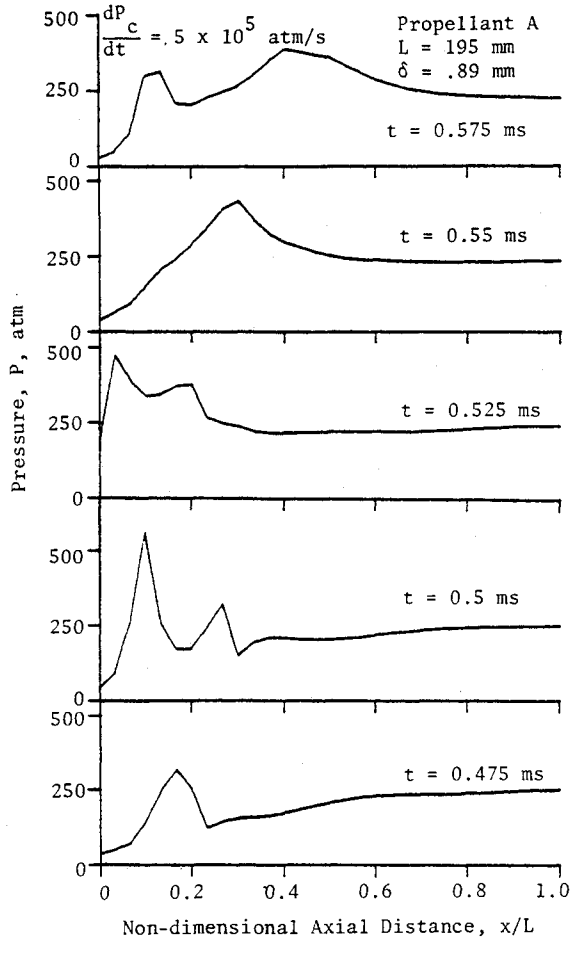

Fig. 13 Calculated pressure distribution at various times during crack-gap closure.

phenomena was taken into account by considering 1) transient one-dimensional mass, momentum, and energy conservation equations in the gas phase; 2) a transient, one-dimensional heat conduction equation in the solid phase; and 3) quasistatic deformation of the two-dimensional, linear-viscoelastic propellant crack due to pressure loading. This set of coupled, nonlinear, partial-differential equations was solved numerically. Gasdynamics equations were solved using a finite-difference analysis, and the structure mechanics equation was solved using a finite-element analysis.

Several important observations and conclusions from this study are summarized in the following.

1) Results indicate that coupling between chamber pressurization, crack combustion, and propellant deformation is quite important, especially in the case of very narrow cracks, and for high chamber pressurization rates.

2) Several regions of partial gap closures were observed experimentally in narrow cracks. Calculated results show that these partial closures may generate substantial local pressure peaks along the crack. The gap closures generally do not occur in the case of large gap widths or low chamber pressures.

3) The initial flame-spreading process, or the time for the ignition front to reach the crack tip, is not affected substantially by propellant deformation. However, structural deformation may significantly affect pressure distributions along the crack.

4) Both theoretical and experimental results show that, in general, the maximum pressure in the crack cavity is higher than that in the chamber.

5) Except near the crack tip region, predicted results for the ignition front propagation are in good agreement with experimental data. Predicted and measured pressure distributions are also in good agreement.

Acknowledgments

This work represents a part of the results obtained under the contract, N00014-79-C-0762, sponsored by the Power Program, Office of Naval Research, Arlington, Va. The support of Dr. Richard S. Miller is appreciated. The assistance of Mr. S. M. Kovacic of The Pennsylvania State University, and Prof. T. Y. Chang and Mr. J. P. Chang of The University of Akron is acknowledged.

References

[1] Price, E. W., ed., *Proceedings of the ONR/AFOSR Workshop on Deflagration to Detonation Transition,* Atlanta, Ga., CPIA Pub., 299.

[2] Kumar, M., Kovacic, S. M., and Kuo, K. K., "Flame Propagation and Combustion Processes in Solid Propellant Cracks," *AIAA Journal,* Vol. 19, May 1981, pp. 610-618.

[3] Kumar, M., "A Study of Flame Spreading and Combustion Processes in Solid Propellant Cracks," Ph.D. Thesis, The Pennsylvania State Univ., Aug. 1980.

[4] Bradley, H. H. Jr. and Boggs, T. L., "Convective Burning in Propellant Defects: A Literature Review," Naval Weapons Center, China Lake, Calif., NWC TP 6007, Feb. 1978.

[5] Belyaev, A. F., Bobolev, V. K., Korotkov, A. I., Sulimov, A. A., and Chuiko, S. V., *Transition from Deflagration to Detonation in Condensed Phases,* translated from Russian by Israel Program of Scientific Translations, Jerusalem, 1975.

[6] Kuo, K. K., Chen, A. T., and Davis, T. R., "Convective Burning in Solid-Propellant Cracks, *AIAA Journal,* Vol. 16, June 1978, pp. 600-607.

[7] Kumar, M. and Kuo, K. K., "Ignition of Solid Propellant Crack Tip Under Rapid Pressurization," *AIAA Journal,* Vol. 18, July 1980, pp. 825-833.

[8] Kumar, M. and Kuo, K. K., "Flame Spreading and Combustion in Solid Propellant Cracks," Final Report to the Naval Weapons Center, China Lake, Calif., July 1980.

[9] Kuo, K. K., Kumar, M., Kovacic, S. M., Wills, J. E., and Chang, T. Y., "Combustion Processes in Solid Propellant Cracks," Naval Weapons Center, China Lake, Calif., NWC TP 6278, June 1981.

[10] Kuo, K. K., Kovalcin, R. L., and Ackman, S. J., "Convective Burning in Isolated Solid Propellant Cracks," Naval Weapons Center, China Lake, Calif., NWC TP 6049, Feb. 1979.

[11] Belyaev, A. F., Korotkov, A. I., Sulimov, A. A., Sukoyan, M. K., and Obmenin, A. V., "Development of Combustion in an Isolated Pore," *Combustion, Explosion, and Shock Waves,* Vol. 5, March 1969, pp. 4-9.

[12] Belyaev, A. F., Bobolev, V. K., Korotkov, A. I., Sulimov, A. A., and Chuiko, S. V., "Development of Burning in a Single Pore," *Transition of Combustion of Condensed Systems to Detonation,* Chap. 5, Pt. A, Sec. 22, Science Publisher, 1973, pp. 115-134.

[13] Kim, K., "Effect of Propellant Crack Burning on High Energy Propellant Safety," *Proceedings of the 16th JANNAF Combustion Meeting,* Monterey, Calif., CPIA Pub. 308, Dec. 1979, pp. 121-141.

[14] Pilcher, D. T., "Modeling the DDT Process," *Proceedings of the ONR/AFOSR Workshop on Deflagration-to-Detonation Transition,* Altanta, Ga., CPIA Pub. 299, Sept. 1978, pp. 143-160.

[15] Kirsanova, Z. V. and Leipunskii, O. I., "Investigation of the Mechanical Stability of Burning Cracks in a Propellant," *Combustion, Explosion, and Shock Waves,* Vol. 6, No. 1, 1970, pp. 68-75.

[16] Cherepanov, G. P., "Combustion in Narrow Cavities," *Journal of Applied Mechanics and Technical Physics,* Vol. 11, No. 2, 1970, pp. 276-281.

[17] Belyaev, A. F., Sukoyan, M. K., Korotkov, A. I., and Sulimov, A. A., "Consequences of the Penetration of Combustion into an Individual Pore," *Combustion, Explosion, and Shock Waves,* Vol. 6, April-June 1970, pp. 149-153.

[18] Williams, M. L. and Jacobs, H. R., "The Study of Crack Criticality in Solid Rocket Motors," Air Force Rocket Propulsion Laboratory, Edwards, Calif., AFRPL-TR-71-21, Jan. 1971.

[19] Jacobs, H. R., Williams, M. L., and Tuft, D. B., "An Experimental Study of the Pressure Distribution in Burning Flaws in Solid Propellant Grains," Air Force Rocket Propulsion Laboratory, Edwards, Calif., AFRPL-TR-72-108, Oct. 1972.

[20] Jacobs, H. R., Hufferd, W. L., and Williams, M. L., "Further Studies of the Critical Nature of Cracks in Solid Propellant Grains," Air Force Rocket Propulsion Laboratory, Edwards, Calif., AFRPL-TR-75-14, March 1975.

[21] Francis, E. C., Lindsey, G. J., and Parmerter, R. R., "Pressurized Crack Behavior in Two-Dimensional Rocket Motor Geometries," *Journal of Spacecraft and Rockets,* Vol. 9, June 1972, pp. 415-419.

[22] Francis, E. C. and Jacobs, H. R., "Fracture Considerations for Surveillance Programs," *Journal of Spacecraft and Rockets,* Vol. 13, Aug. 1976, pp. 451-455.

[23] Takata, A. N. and Wiedermann, A. H., " Initiation Mechanism of Solid Rocket Propellant Detonation," IIT Research Institute, Chicago, Ill., Interim Reports for AFOSR, Aug. 1976-Nov. 1979.

[24] Takata, A. N. and Wiedermann, A., "Initiation Mechanism of Solid Rocket Propellant Detonation," 14th JANNAF Combustion Meeting, Monterey, Calif., CPIA Pub. 292, Dec. 1977.

[25] Knauss, W. G., "Stable and Unstable Crack Growth in Viscoelastic Media," *Transactions of the Society of Rheology,* Vol. 13, 1969, pp. 291-313.

[26] Knauss, W. G. and Dietmann, H., "Crack Propagation Under Variable Load Histories in Linearly Viscoelastic Solids," *International Journal of Engineering Sciences,* Vol. 8, Aug. 1970, pp. 643-656.

[27] Schapery, R. A., "A Theory of Crack Initiation and Growth in Viscoelastic Media, I. Theoretical Development," *International Journal of Fracture,* Vol. 11, Feb. 1975, pp. 141-159.

[28] Schapery, R. A., "A Theory of Crack Initiation and Growth in Viscoelastic Media, II. Approximate Methods of Analysis," *International Journal of Fracture,* Vol. 11, June 1975, pp. 369-388.

[29] Schapery, R. A., "A Theory of Crack Initiation and Growth in Viscoelastic Media, III. Analysis of Continuous Growth," *International Journal of Fracture,* Vol. 11, Aug. 1975, pp. 549-562.

[30] Nuismer, R. J., "On the Governing Equation for Quasi-Static Crack Growth in Linearly Viscoelastic Materials," *Journal of Applied Mechanics,* Vol. 41, 1974, pp. 631-634.

[31] Jacobs, H. R., Hufferd, W. L., and Liem, K., "On a Fracture Growth Criterion for Viscoelastic Materials," Univ. of Utah, Salt Lake City, Utah, UTEC CE 74-102, July 1974.

[32] Beckinth, S. W. and Wang, D. T., "Crack Propagation in Double-Base Propellants," *Journal of Spacecraft and Rockets,* Vol. 15, Nov.-Dec. 1978, pp. 355-361.

[33] Langlois, G. and Gonard, R., "New Law for Crack Propagation in Solid Propellant Material," *Journal of Spacecraft and Rockets,* Vol. 16, Nov.-Dec. 1979, pp. 357-360.

[34] Swanson, S. R., "A Cohesive Crack Tip Model for Dynamic Viscoelastic Fracture," Univ. of Utah Report, 1977.

[35] Courant, R. and Hilbert, D., *Methods of Mathematical Physics,* Vol. 2, Interscience Publishers, New York, July 1966, pp. 407-550.

[36] Peretz, A., "The Starting Transient of Solid Propellant Rocket Motors with High Internal Gas Velocities," Ph. D. Thesis, AMS Dept., Princeton Univ., April 1973.

[37] Peretz, A., Kuo, K. K., Caveny, L. H., and Summerfield, M., "Starting Transient of Solid-Propellant Rocket Motors with High Internal Gas Velocities," *AIAA Journal,* Vol. 11, Dec. 1973, pp. 1719-1727.

[38] Svehla, R. A., "Estimated Viscosities and Thermal Conductivities of Gases at High Temperatures," NASA TR R-132, 1962.

[39] Bartz, D. R., "Survey of the Relationship Between Theory and Experiment for Convective Heat Transfer from Rocket Combustion Gases," *Advances in Tactical Rocket Propulsion,* AGARD Conference Proceedings No. 1, Technivision Services, Maidenhead, England, Aug. 1968, pp. 291-381.

[40] Hilsenrath, J. et al., "Tables of Thermal Properties of Gases," U. S. Dept. of Commerce, NBS Cir. 564, Nov. 1955.

[41] Colebrook, C. F., "Turbulent Flow in Pipes with Particular Reference to the Transition Region Between the Smooth and Rough Pipe Laws," *Journal of the Institute of Civil Engineers,* Vol. 11, 1938-39, pp. 133-156.

[42] Schlichting, H., "Turbulent Flow Through Pipes," *Boundary Layer Theory,* 6th Ed., McGraw-Hill, New York, 1968.

[43] Razdan, M. K. and Kuo, K. K., "Measurements and Model Validation for Composite Propellants Burning Under Cross Flow Conditions," *AIAA Journal,* Vol. 18, June 1980, pp. 669-677.

[44] Lenoir, J. M. and Robillard, G., "A Mathematical Method to Predict the Effects of Erosive Burning in Solid Propellant Rockets," *6th Symposium (International) on Combustion,* The Combustion Institute, Pittsburgh, Pa., 1956, pp. 663-667.

[45] Vichnevetsky, R. and Tomalesky, A. W., "Spurious Wave Phenomena in Numerical Approximations of Hyperbolic Equations," *Proceedings of the Fifth Annual Princeton Conference on Information Science and Systems,* Princeton Univ., March 1971, pp. 1-7.

[46] Chang, T. Y. and Prachuktam, S., "NFAP—A Nonlinear Finite Element Analysis Program," Rept. SE 76-3, Dept. of Civil Engineering, Univ. of Akron, Akron, Ohio, Oct. 1976.

[47] Bathe, K. J. and Wilson, E. L., "NONSAP—A Nonlinear Structural Analysis Program," *Nuclear Engineering and Design,* Vol. 29, No. 2, 1974, pp. 266-293.

[48] Bathe, K. J., Wilson, E. L., and Iding, R. H., "NONSAP: A Structural Analysis Program for Static and Dynamic Response of Nonlinear Systems," Univ. of California, Berkeley, Calif., USEMS 74-3 (also NTIS PB-231 112), Feb. 1974.

[49] Chang, T. Y., Chang, J. P., Kumar, M., and Kuo, K. K., "Combustion-Structural Interaction in a Viscoelastic Material," *Symposium on Computational Methods in Nonlinear Structural and Solid Mechanics,* NASA CP 2147, Oct. 1980, pp. 67-90.

[50] Price, C. F., private communication, Naval Weapons Center, China Lake, Calif., Jan. 1978.

[51] Gordon, S. and McBride, B. J., "Computer Program for Calculation of Complex Chemical Equilibrium Compositions, Rocket Performance, Incident and Reflected Shocks, and Chapman-Jouguet Detonations," NASA SP-273, 1971.